Development of a Terrain Adaptive Stability Prediction System for Mass Articulating Mobile Robots

Antonio Diaz-Calderon¹, Alonzo Kelly
The Robotics Institute
Carnegie Mellon University
Pittsburgh, PA 15213

Abstract

Dynamic stability is an important issue for vehicles which move heavy loads, turn at speed, or operate on sloped terrain. In many cases, vehicles face more than one of these challenges simultaneously. This paper presents a methodology for deriving proximity to tipover for autonomous field robots which must be productive, effective, and self reliant under such challenging circumstances. The technique is based on explicit modelling of mass articulations and determining the motion of the center of gravity, as well as the attitude, in an optimal estimation framework. Inertial sensing, articulation sensing, and terrain relative motion sensing are employed. The implementation of the approach on a commercial industrial lift truck is presented.

1 Introduction

This paper addresses the issue of detecting proximity to a tipover event for an articulating mobile robot subject to large inertial accelerations. Articulating mobile robots can alter their configuration in response to commands issued to move the payload. As a result, the location of the center of mass (cg) of the vehicle is not fixed; a characteristic that may adversely affect the maneuverability of the vehicle. In this work, the general idea of computing the instantaneous motion of the cg of the vehicle relative to an inertial reference frame is addressed first. Following this, an algorithm to quantify the stability regime of the vehicle based on the inertial forces acting on the vehicle as a result of induced accelerations is presented. This algorithm is based on the assumption that the internal D'Alembert forces are negligible

1.1 Related work

Study of rollover phenomena for heavy trucks abound in the automotive literature e.g., [1, 4, 5, 10, 12]. These authors study lateral rollover propensity under different handling conditions. While the proposed static characterizations of vehicle lateral stability are not appropriate as instantaneous measures of vehicle stability they do highlight the importance of considering the height of the cg and the vehicle weight. Another important property that limits the applicability of these results to our problem is the fact that heavy trucks do not articulate any mass.

Articulating mobile robots on the other hand can change their configuration affecting the location of their cg. For these systems researchers have proposed a number of approaches [3, 7, 8, 9, 11] that can be broadly classified as quasi-static stability approaches. In a quasi-static approach it is assumed that the vehicle motion relative to an inertial reference frame is slow (e.g., 1 m/s or less), therefore inertial accelerations can be neglected with the exception of gravitational acceleration. As a result, the vehicle does not experience inertial forces that might trigger the tipover event. Approaches based on the support polygon are presented in [7, 9, 11]. These approaches suffer from the common problem of not measuring true cg motion while still assuming slow velocities. For vehicles that can articulate significant mass over long distances, and experience significant inertial accelerations, the quasi-static stability assumption is not applicable.

1.2 Approach

In this paper, the instantaneous motion of the cg is computed together with the inertial forces acting on the cg as a result of this motion. Sensor indications are mapped onto the instantaneous location of the cg providing true cg motion.

To evaluate the stability regime of the vehicle, two derived vehicle states are defined: motion state and configuration state. The former provides information as to what the vehicle is doing (i.e., how fast it is turning, is it driving on a non-level road, how heavy is the load, etc.) and the latter provides information as to the configuration of the articulated parts at any point in time. The configuration state of the vehicle determines the limits on the D'Alembert forces that can be applied to the vehicle without actually causing a tipover event. It is also used to compute the instantaneous

^{1.} Corresponding author.

location of the vehicle cg relative to its polygon of support. The location of the cg (in 3D space) along with the inertial forces acting on the vehicle enable the computation of the *tipover stability regime*, which is a measure of the proximity of the vehicle to a tipover event as a function of motion and configuration states.

The proposed stability algorithm consists of two parts:
1) an estimation and prediction system and 2) a dynamic module. The estimation and prediction system estimates the current and future states of the vehicle using on-board sensors to measure relevant dynamic quantities. The dynamic module computes the stability regime using the vehicle's state estimate.

The utility of a tipover proximity indicator is that it can be used to drive a number of mechanisms which can take corrective action. For man-driven vehicles, a console indication or audible warning could be produced. For autonomous systems, an exception can be raised for resolution at higher levels of the autonomous hierarchy or various governing mechanisms can be engaged to actively reduce the severity of the situation.

This paper is organized as follows: Section 2 presents the optimal estimation framework, Section 3 presents our approach to assessing the stability regime of the vehicle and Section 4 presents some results from the application of the algorithms presented in the paper.

2 Optimal estimation framework

The estimation and prediction system provides the instantaneous motion of the vehicle cg using on-board sensors to measure relevant dynamic quantities. This framework is based on an extended Kalman filter (EKF) [6].

2.1 System Dynamics

The system's state vector describes the motion of the cg of the vehicle as well as the vehicle attitude:

$$\mathbf{x} = \begin{bmatrix} \mathbf{v} & \mathbf{a} & \mathbf{\omega}_z & \mathbf{\alpha}_z & \mathbf{\phi} & \mathbf{\theta} \end{bmatrix}^T$$
 Eq. 1

where \mathbf{v} and \mathbf{a} are the linear velocities and accelerations of the cg, and ω_z and α_z are the angular velocities and accelerations of the cg about the vehicle's vertical, and ϕ and θ are the Euler angles that describe the vehicle attitude.

The system dynamics will be described by the following differential equation:

$$f(\mathbf{x}) = \begin{bmatrix} \mathbf{a} & \mathbf{0}_{3 \times 1} & \alpha_z & 0 & \frac{\sin(\theta)\cos(\phi)\omega_z}{\cos(\theta)} & -\sin(\phi)\omega_z \end{bmatrix}^{\mathrm{T}} \text{Eq. 2}$$

This system model is nonlinear, therefore given the initial condition $\mathbf{x} = \mathbf{x}_k$ at time t_k we use the formula for the Euler method (Eq. 3) to advance the solution of the nonlin-

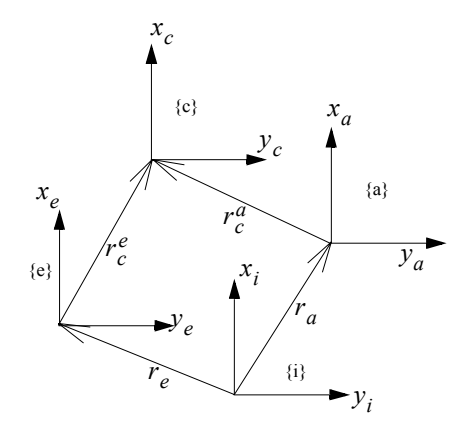


Figure 1: Frames used in the transformation of sensor data.

ear differential equation $\dot{\mathbf{x}} = f(\mathbf{x})$ from t_k to $t_{k+1} = t_k + dt$.

$$\mathbf{x}_{k+1} = \mathbf{x}_k + f(\mathbf{x}_k)dt$$
 Eq. 3

2.2 Measurements

We are interested in the true motion of the cg because that motion determines the instantaneous stability regime (e.g., stable, marginally stable) of the vehicle. However, sensor indications describe the sensor's own motion. To find the true cg motion, sensor indications are mapped onto sensor indications at the cg taking into account the motion of the cg relative to the sensor.

Transformation of inertial sensor measurement. With

reference to Fig. 1, let frame {i} be the inertial reference frame attached to the earth, frame {e} be a frame attached to the encoder sensor, frame {a} be attached to the accelerometer, and frame {c} be attached to the cg of the vehicle. The relative motion between these frame is constrained as follows: $\vec{\omega}_a^c = \vec{\omega}_a^e = \vec{\omega}_c^e = 0$, $\vec{v}_a^e = 0$, $\vec{v}_c^e \neq 0$, and $\vec{v}_c^a \neq 0$.

With this frame definitions, the speed of the cg (i.e., \dot{v}_c) relative to the inertial frame is computed from Eq. 4 as follows.

$$\dot{\hat{v}}_c = \left(\frac{d\hat{r}_c}{dt}\right)_i = \dot{\hat{v}}_e + \dot{\hat{v}}_c^e + \dot{\hat{\omega}}_e \times \dot{\hat{r}}_c^e$$
 Eq. 4

We use the symbols \mathring{r}_c^n and \mathring{v}_c^n to describe the position and velocity of the cg relative to the *nth* sensor.

The specific force, t_c , measured at the cg is computed from $t_c = t_a + \Delta t$, where t_a is the specific force measured

by the accelerometer and $\Delta \hat{t}$ is an increment in specific force due to the offset of the cg relative to the accelerometer. This increment can be computed from Eq. 5 as follows:

$$\Delta \dot{t} = \dot{a}_c^a + 2\dot{\omega}_a \times \dot{v}_c^a + \dot{\alpha}_a \times \dot{r}_c^a + \dot{\omega}_a \times \dot{\omega}_a \times \dot{r}_c^a \qquad \text{Eq. } 3$$

The location and motion of the cg relative to the sensor induce inertial accelerations that must be accounted for when measuring true cg motion. Induced inertial accelerations are the following:

Acceleration seen in frame {a}
$$\dot{a}_c^a$$

Euler acceleration $\dot{\alpha}_a \times \dot{r}_c^a$

Coriolis acceleration $2\dot{\omega}_a \times \dot{V}_c^a$

Centripetal acceleration $\dot{\omega}_a \times \dot{\omega}_a \times \dot{r}_c^a$

where $\vec{\omega}_a$ and $\vec{\alpha}_a$ are the angular velocity and acceleration (about the local vertical) of the sensor.

Kinematics of the CG. As the robot is articulated, the cg experiences additional velocities and accelerations relative to the inertial frame. To account for these velocities and accelerations, we compute the instantaneous motion of the cg relative to the body frame. The sensor transformations derived earlier are then applied to obtain the true cg motion.

$${}^{B}\mathbf{r}_{c} = {}^{B}_{0}\mathbf{T} \left({}^{0}\mathbf{r}_{c_{0}}m_{0} + \sum_{i=1}^{n} \left(\prod_{j=1}^{i} {}^{j-1}_{j}\mathbf{T}(\Theta_{j}) \right)^{i}\mathbf{r}_{c_{i}}m_{i} \right) \frac{1}{m} \quad \text{Eq. 6}$$

Eq. 6 defines the instantaneous location of the cg $({}^B\mathbf{r}_c)$ as a function of joint variables Θ_i .

Measurement model. The measurement z includes: yaw rate gyro (ω), steer encoder (δ), speed (ν), accelerometers specific force (t), and roll (Φ) and pitch (Θ) inclinometers.

$$\mathbf{z} = \begin{bmatrix} z_{\omega} & z_{\delta} & z_{v_x} & z_{v_z} & z_{v_z} & z_{t_a} & z_{\Phi} & z_{\Theta} \end{bmatrix}^T$$
Eq. 7

Eq. 8 gives the relationship between the state x and z, which is non-linear. The measurement Jacobian is defined

as
$$\mathbf{H} = \frac{\partial \mathbf{h}}{\partial \mathbf{x}}$$
 and the matrix $_{B}^{i}\mathbf{R} = \mathbf{R}_{z}(0)\mathbf{R}_{y}(\theta)\mathbf{R}_{x}(\phi)$ is

the ZYX-Euler angles rotation matrix that describes the orientation of the truck relative to the earth, and ${}^{B}_{i}\mathbf{R} = ({}^{i}_{B}\mathbf{R})^{-1}$.

$$\operatorname{atan}\left(\frac{v_{y}-v_{c_{y}}^{\delta}-\omega_{z}r_{c_{x}}^{\delta}}{v_{x}-v_{c_{x}}^{\delta}+\omega_{z}r_{c_{y}}^{\delta}}\right)$$

$$v_{x}-v_{c_{x}}^{e}+\omega_{z}r_{c_{x}}^{e}$$

$$v_{z}-v_{c_{z}}^{e}$$

$$\mathbf{a}+\frac{B}{i}\mathbf{R}^{i}\mathbf{g}-\Delta\mathbf{t}_{a_{s}}$$

$$\operatorname{atan}\left(\frac{-(\mathbf{a}+\frac{B}{i}\mathbf{R}^{i}\mathbf{g}-\Delta\mathbf{t}_{\mathrm{inc}_{s}})_{y}}{(\mathbf{a}+\frac{B}{i}\mathbf{R}^{i}\mathbf{g}-\Delta\mathbf{t}_{\mathrm{inc}_{s}})_{z}}\right)$$

$$\operatorname{atan}\left(\frac{(\mathbf{a}+\frac{B}{i}\mathbf{R}^{i}\mathbf{g}-\Delta\mathbf{t}_{\mathrm{inc}_{s}})_{z}}{(\mathbf{a}+\frac{B}{i}\mathbf{R}^{i}\mathbf{g}-\Delta\mathbf{t}_{\mathrm{inc}_{s}})_{z}}\right)$$

3 Assessment of stability regime

Assessing stability regime is accomplished in two steps. First, the geometric footprint of the vehicle is computed. This is used to determine the limits on the motion of the cg; i.e., stability envelope. Second, the forces acting on the cg are determined. These forces are used to formulate a single stability measure of the vehicle's stability regime, which is expressed as an angle measure.

Definition of the support polygon. The polygon of support is defined by the robot contact points with the ground, which form a convex polygon when projected onto the horizontal plane. For example, in a wheeled vehicle these contact points may be defined by the center of the contact patch of the tire and the road. Let \hat{r}_i represent the location of the ith ground contact point and let \dot{r}_c represent the location of the vehicle center of mass. As illustrated in Fig. 2 these vectors can be expressed in the vehicle frame {B} and numbered such that the unit normal of the support polygon is directed upward and out of the ground. The boundary of the support polygon is defined by the lines joining the ground contact points. These lines are the candidate tipover axes, \hat{a}_i , i = 1...n. The *ith* tipover axis is the axis about which the vehicle will physically rotate during a tipover event. It defines the normal to the tipover plane (Figure 2). The tipover plane serves as a simplification in which the vehicle mass properties and the forces acting on the vehicle are projected onto to analyze the tipover propensity about the plane normal.

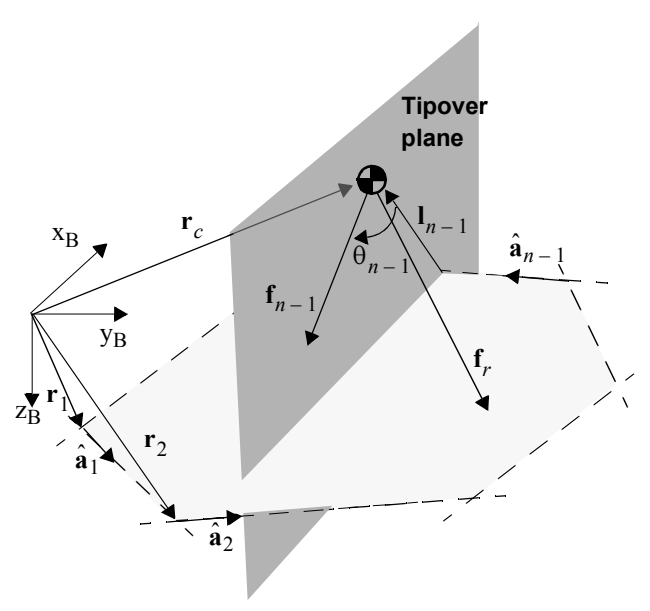


Figure 2: Assessment of dynamic stability.

Formulation of the stability measure. The sum of forces acting on the vehicle must be balanced when the vehicle is in a stable configuration. These forces include the inertial forces ($\hat{f}_{inertial}$), gravitational loads (\hat{f}_g), ground reaction forces at the vehicle's wheels (\hat{f}_s), and any other external disturbances acting on the vehicle (\hat{f}_d). The force equilibrium equation can be written as in Eq. 9.

$$\sum_{i=1}^{\infty} \hat{f}_{inertial} = \sum_{i=1}^{\infty} (\hat{f}_g + \hat{f}_s + \hat{f}_d)$$
 Eq. 9

The net force acting on the cg that would contribute to tipover instability about any tipover axis, \dot{f}_r , is defined in Eq. 10.

$$\dot{f}_r \stackrel{\Delta}{=} \sum (\dot{f}_g + \dot{f}_d - \dot{f}_{inertial}) = -\sum \dot{f}_s$$
 Eq. 10

For a given tipover axis \hat{a}_i , we are only concerned with those components of \hat{f}_r , which act *about* the *ith* tipover axis. The projection of the resultant force onto the *ith* tipover plane and the moment of the resultant force about the plane normal are used to compute the stability measure as follows.

Let f_i be the projection (e.g., the component of f_r acting along the *ith* tipover axis) of the resultant force onto the tipover plane. Then

$$\dot{f}_i = \dot{f}_r - (\dot{f}_r \cdot \hat{a}_i) \hat{a}_i$$
 Eq. 11

and $\hat{a}_i = \frac{1}{a_i}/|\hat{a}_i|$. Similarly, the torque acting about the *ith* tipover axis can be computed from Eq. 12.

$$\hat{n}_i = ((\hat{l}_i \times \hat{f}_r) \cdot \hat{a}_i)\hat{a}_i$$
 Eq. 12

In Eq. 12, l_i is the *ith* tipover axis normal given by

$$\dot{l}_i = (\dot{p}_i - \dot{p}_c) - ((\dot{p}_i - \dot{p}_c) \cdot \hat{a}_i)\hat{a}_i$$

The stability measure for each tipover axis is defined as the subtended angle between the *ith* resultant force, \vec{f}_i , and the *ith* tipover axis normal, λ_i , as illustrated in Figure 2. This measure is denoted by θ_i and can be computed from Eq. 13 as follows:

$$\theta_i = -\operatorname{asin}\left(\frac{(\hat{l}_i \times \hat{f}_r) \cdot \hat{a}_i}{|\hat{l}_i||\hat{f}_i|}\right)$$
 Eq. 13

The stability regime with respect to a given tipover axis is determined from the value of the corresponding resultant angle as follows. If the resultant angle $\theta_i > 0$ the vehicle is stable about the *ith* tipover axis. If $\theta_i = 0$ the vehicle is marginally stable about that tipover axis. This means that the ground reaction forces at the inside support points relative to the *ith* tipover axis are zero. If $\theta_i < 0$ the vehicle is critically stable, meaning that it is tipping over about the *ith* tipover axis. The overall stability regime of the vehicle is defined by Eq. 14.

$$\theta = \min(\theta_i)$$
 Eq. 14

4 Results

The testbed selected to exercise the algorithm is a lift truck. Two platforms were used in testing the algorithm: hardware and simulation. The hardware platform is shown in Fig. 3 and Fig. 4. A commercial lift truck underwent major retrofitting to incorporate the sensor suite used in the system.

There are two types of sensors used in the system: inertial and articulation. Inertial sensors measure inertial motion and direction of gravity. Articulation sensors measure motion of every articulated part of the vehicle.

The computing platform is a general purpose 3U form factor 8-slot chassis containing a backplane for PXI and Compact PCI modules. The CPU module is a National Instruments PXI-8170 series consisting of a 850 MHz Pentium III processor with 256 MB of memory.

As part of the hardware platform, a data logger system was developed. The main function of the logger is to provide input data to the system from either the vehicle sensors, from previously generated log files or from simulated sensor data. In the design of the logger, care was taken to



Figure 3: Vehicle test bed.



Figure 4: Vehicle test bed: mast extended to 340 inch high.

guarantee deterministic log play back to ensure identical system response regardless of the source of the input data.

Experiments to verify the functionality of the system involved driving the vehicle on ramps, and level ground. Different handling maneuvers were executed, e.g., constant curvature/constant speed/changing load location, constant

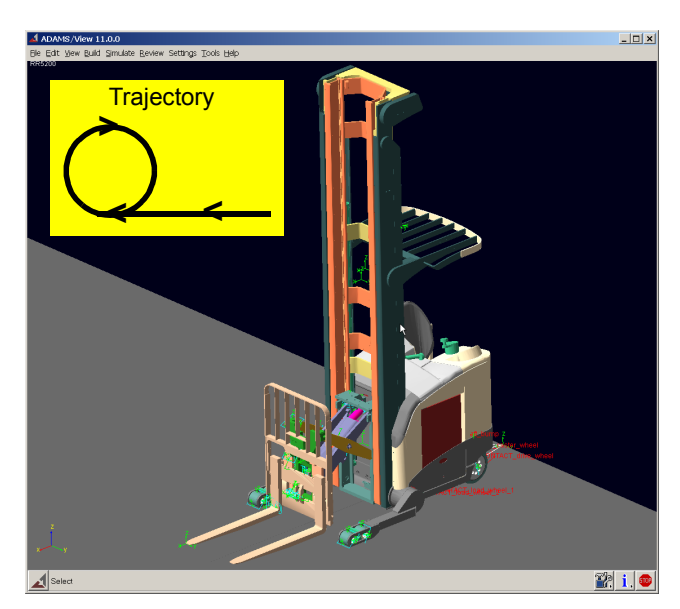


Figure 5: Rigid body dynamic model of the test bed. The trayectory executed is shown in the inset.

curvature/variable speed, variable curvature/variable speed. Testing on ramps was important to verify if the system was able to decouple inertial accelerations due to motion from gravity: inclinometers and accelerometers are unable to make the distinction. In all these cases, the system estimated the attitude of the vehicle (e.g., terrain grade) to within one degree and was able to compute the stability measure by decoupling inertial accelerations from gravity.

More aggressive maneuvers were left to be tested in simulation. The simulation environment is based on rigid body dynamic models of the truck, which have been developed in ADAMS [2] (Fig. 5).

A test run was executed with a trajectory composed of two sections: acceleration section and maneuver section. A linear path is used to accelerate the vehicle to the commanded speed (5 m.p.h). This is followed by a constant curvature path with variable longitudinal velocity (5—>10 m.p.h.). This is illustrated in the inset in Figure 5. The maneuver was executed while the vehicle was carrying a load of 3000 lb. Simulated sensor indications for this maneuver are illustrated in Fig. 6 while estimated velocities and accelerations at the cg of the vehicle are illustrated in Fig. 7.

As the vehicle travels in this constant curvature path, the longitudinal velocity of the truck is increased to 10 m.p.h. This causes an increase in lateral acceleration as illustrated in Fig. 7. As a result, the resultant angles that correspond the outside tipover axes decrease to a point where the truck has reached marginal stability: the resultant angle (theta_2) in Fig. 9 goes to zero. It is at this point where the vehicle's inside wheels are about to lift-off the ground. Verifying the reaction forces at the wheels (Fig. 8),

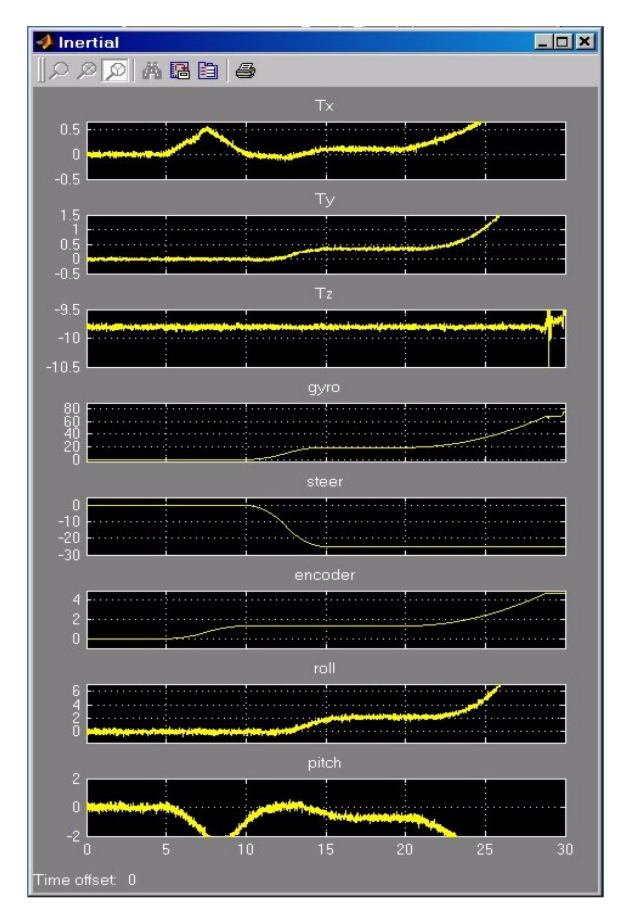


Figure 6: Simulated sensor indications. Tx, Ty, and Tz represent accelerometer specific force. Roll and pitch are the outputs of the simulated inclinometers. As the vehicle travels the constant curvature path the roll inclinometer is unable to differentiate between gravity or inertial acceleration due to motion.

we confirm that the reaction forces on the inside wheels become zero.

5 Conclusions

This paper has presented an approach to estimating proximity to tipover for a case much more general than previous approaches. The technique applies to vehicles which articulate significant mass, which experience significant inertial forces, and which move over terrain which is not necessarily level. Key elements of the approach include explicit models of mass articulation, an optimal estimation approach to motion determination, explicit compensation for inertial forces, and a formulation that determines the motion of the cg frame of reference.

The generality of the approach makes it potentially relevant to a broad class of outdoor material handling and excavation vehicles whether they are man-driven or robotic. The system could form the basis of a governing system which

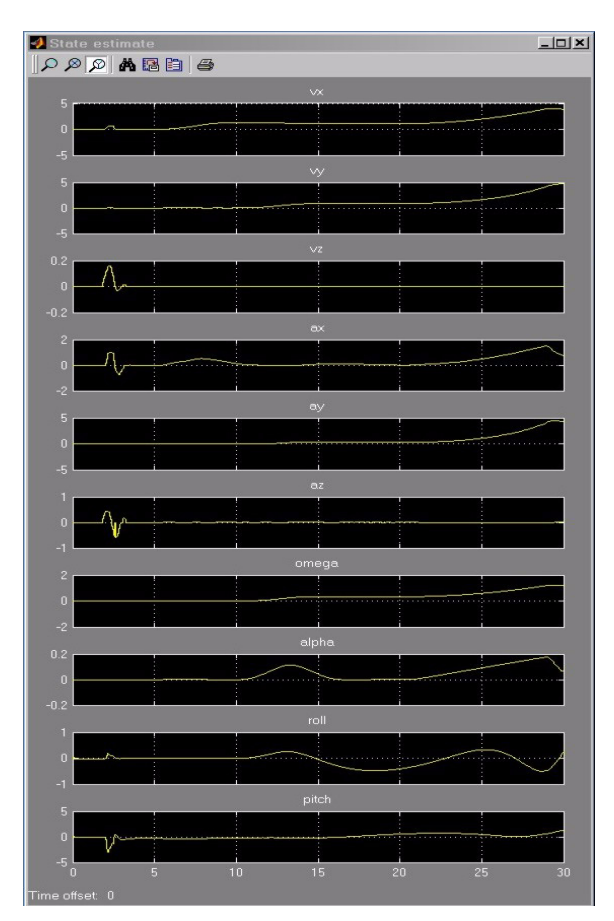


Figure 7: Vehicle cg state. As the vehicle enters the constant curvature path, lateral velocity and acceleration are being estimated. Lateral acceleration is used in the stability measure to monitor the lateral stability of the vehicle within its stability envelope. The attitude of the vehicle is given by the roll and pitch angle outputs.

discourages aggressive driving for man-driven vehicles or one which implements a low level reactive control system for an autonomous vehicle.

References

- [1] "Mechanics of heavy-duty trucks and truck combinations," Transportation Research Institute, The University of Michigan, Ann Arbor, MI, Engineering Summer Conferences UMTRI-80868, 1991.
- [2] ADAMS, Mechanical Dynamics Inc., Ann Arbor, MI, 2001.
- [3] Dubowsky S. and E. E. Vance, "Planning mobile manipulator motions considering vehicle dynamic stability constraints," in IEEE International Conference on Robotics and Automation, Scottsdale, AZ, May 1989.
- [4] Genta, G., *Motor vehicle dynamics*. Series on Advances in Mathematics for Applied Sciences.

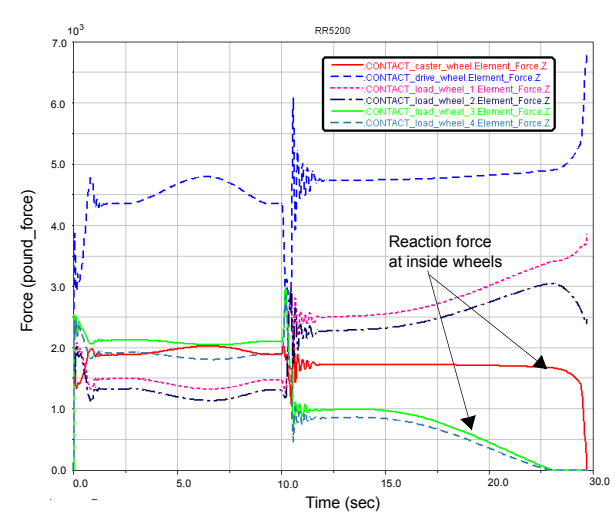


Figure 8: Wheel reaction forces. Wheel reaction forces for the inside wheels go to zero as the vehicle reaches marginal stability.

Vol. 43. 1999, Singapore: World Scientific Publishing.

- [5] Gillespie T. D., Fundamentals of vehicle dynamics. Warrendale, PA: Society of Automotive Engineers, 1992.
- [6] Maybeck P. S., Stochastic models, estimation and control. Academic Press, 1982.
- [7] Papadopoulos E.G. and D. A. Rey, "A new measure of tipover stability margin for mobile manipulators," Proceedings of the 1996 IEEE International Conference on Robotics and Automation, Minneapolis, MN, April 1996.
- [8] Shiller Z. and Y. R. Gwo, "Dynamic motion planning of autonomous vehicles," IEEE Transactions on Robotics and Automation, vol 7, April 1991.
- [9] Sreenivasan S. V. and B. H. Wilcox, "Stability and traction control of an actively actuated micro-rover," Journal of Robotics Systems, vol. 11 no. 6, 1994.
- [10] Steiner, P., et al., *Rollover detection*. SAE Paper no. 970606, 1997.
- [11] Sugano S, Q. Huang and I Kato, "Stability criteria in controlling mobile robotic systems," in IEEE Inter-

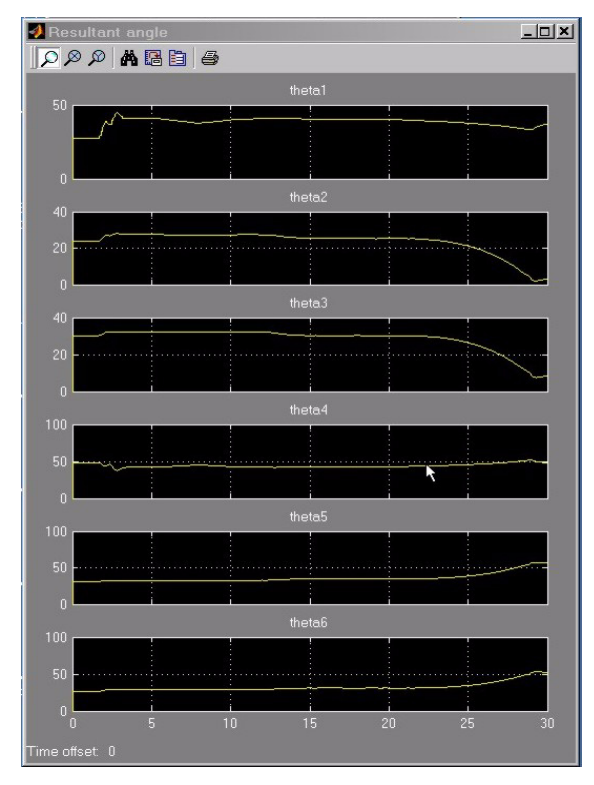


Figure 9: Stability regime expressed as the angle of the resultant. This vehicle has six candidate tipover axes hence the six resultant angles. Resultant angles associated with the tipover axes 2 and 3 decrease since these axes are the candidate tipover axes for this maneuver. Axes 5 and 6 are on the opposite side therefore their associated angles increase. Finally, axes 1 and 4 correspond to the front and rear tipover axes (e.g., longitudinal tipover).

- national Workshop on Intelligent Robots and Systems, Yokohama, Japan, July 1993.
- [12] Winkler C. B., D. Blower, R. D. Ervin and R. M. Chalasani, *Rollover of heavy commercial vehicles*. Warrendale, PA: Society of Automotive Engineers, 2000.